View metadata, citation and similar papers at core.ac.uk
brought to you by CORE
provided by NOPR

Indian Journal of Pure & Applied Physics
Vol. 58, March 2020, pp. 147-156

Energy efficient decision fusion for differential space-time block codes in wireless sensor networks

M Kanthimathi[a]*, R Amutha[b], D Vaithiyanathan[c] & S Somesh Sharma[d]

[a]Department of Electronics and Communication Engineering, Sri Sairam Engineering College, Chennai 600 044, India

[b]Department of Electronics and Communication Engineering, S S N College of Engineering, Chennai 603 110, India

[c]Department of Electronics and Communication Engineering, NIT, New Delhi 110 040, India

[d]Department of Electronics and Communication Engineering, Sri Sairam Engineering College, Chennai 600 044, India

Received 4 September 2019; accepted 10 January 2020

The non-coherent techniques that do not require the channel state information have gained significant interest especially when multiple transmitter and receiver nodes are involved in communication. In this paper, we analyze the energy efficiency of differential and coherent cooperative Multiple-input Multiple-output (MIMO) method using space-time block codes (STBC). We exploit the benefits of the extension of the observation interval of differential STBC to three blocks in Wireless sensor networks (WSNs). We propose an energy efficient decision fusion (EEDF) algorithm in WSNs which utilizes the benefits of Multiple symbol differential detection (MSDD) decision fusion by optimally selecting the ring amplitude of the differential amplitude phase shift keying (DAPSK) constellation. The simulation results show that processing differential multiple symbols provides significant energy saving compared to the conventional two-symbol processing. Furthermore, significant performance gain is achieved for the proposed algorithm compared to 16 DPSK MSDD decision fusions.

Keywords: Differential amplitude phase shift keying (DAPSK) constellation, Fast fading channel, Energy minimization, Space time modulation, Wireless sensor network

1 Introduction

Wireless sensor networks can be deployed rapidly and are very useful in military applications, medical applications and environmental applications[1]. Replacement of sensors that have ran out of energy is difficult hence, it is essential to design energy efficient WSN's. Further, the transmission environment may sometimes be significantly degraded causing practical difficulty in tracking and estimating a coherent demodulation reference signal. Therefore, the differential detection technique becomes an attractive alternative to coherent detection especially when it is difficult to acquire channel state information. Differential detection requires additional Signal to noise ratio (SNR) compared to ideal coherent detection. MSDD is proposed in literature[2] for reducing the irreducible error floor associated with conventional differential detection. Interestingly, STBC can achieve full diversity gain without reduction in data rate. Motivated by the benefits of STBC, detailed bit error rate (BER) analysis was carried out in literature[3]. In literature[4], a closed form BER expression was derived for the BER for STBC, employing M-ary phase shift keying modulation with non-coherent differential encoding/decoding. Theoretical results were verified with simulated results of STBC using BPSK and QPSK modulations.

Quasi orthogonal STBC achieves full diversity and also provides good performance at high SNR[5]. A multichannel amplitude phase shift keying modulation (APSK) for space-time communication (STC) was presented in literature[6]. The proposed method provides higher spectral efficiency compared to STC method involving only phase modulation. MSDD schemes for M-ary phase shift keying STBC was presented in literature[7]. The differential transmission scheme greatly narrows the 3-db performance gap compared to coherent transmission. Moreover, the performance of differential space time block codes using non coherent modulus constellations was demonstrated in literature[8]. In literature[9], the probability of error of 16-APSK is theoretically evaluated. They found the optimum ring ratio and the detection threshold that makes the 16-APSK a spectrally efficient transmission scheme in practical mobile fading channels. Furthermore, a low-complexity

*Corresponding author (E-mail: kanthimathi.ece@sairam.edu.in)

soft-decision MSDD using iterative amplitude/phase processing (MSDD-IAP) coded DAPSK was proposed in literature[10]. Reduced complexity near optimal star QAM aided differentially encoded space time shift keying (STSK) scheme was proposed in literature[11].

The total energy required to send a given number of bits through cooperative MIMO transmission was analyzed in literature[12]. Moreover, the authors showed that significant energy saving is possible with cooperative MIMO for transmission distance above certain threshold. They also suggested the best modulation strategy required to minimize the total energy consumed to send a given number of bits. To reduce the energy consumption per unit in the multi-hop virtual MIMO system, a multi-hop virtual MIMO protocol to jointly improve the energy efficiency, reliability and end-to-end (ETE) QoS provisioning in WSN was proposed in literature[13]. The possibility of power efficient solutions using advanced cooperation aided wireless MIMO transceivers were studied extensively in literature[14]. The energy efficiency is improved in the cooperative multi-input-single-output (MISO) configuration in ad hoc networks by optimizing the hop distance[15]. By finding a minimum energy consuming configuration significant energy saving was achieved in multi-hop network[16]. To prolong the lifetime of WSNs a distributed cooperative clustering protocol was designed in literature[17] which use the advantage of virtual MIMO technology. The problem of the decision fusion in WSN's when the channel is fast fading is analyzed in literature[18]. Moreover, significant performance gain was achieved by increasing the observation window to more than two symbol intervals. By optimizing the error probability and the hop distance, the overall energy consumption in a WSN was minimized in literature[20]. Energy efficiency of non-coherent modulation techniques in WSNs were studied extensively. Energy consumption using Unitary space time modulation (USTM) is investigated in literature[21]. Energy minimization is achieved by optimizing the hop distance and the number of cooperating nodes.

Generally, the speed of the mobile node affects the received signal level. The doppler spread increases with increase in speed. In differential modulation there is an irreducible error floor due to doppler spread. In fast fading channel conditions, the channel has less time to decorrelate between transmitted symbols. But as the data rate increases, the bit duration decreases so it appears to be slow fading. In this scenario, the performance of differential modulation increases as data rate increases[18]. Hence, we propose EEDF algorithm using bandwidth efficient DAPSK modulation. Differential schemes are highly beneficial compared to coherent MIMO systems as it avoids channel estimation of all the MIMO channels. Moreover, bandwidth efficient 16 DAPSK modulations perform better compared to 16 DPSK modulation.

Against this background, the novel contributions of this paper are as follows:

(i) Firstly, we derive the energy consumption per bit for cooperative STBC with differential detection using BPSK and QPSK modulation in WSNs. We also demonstrate the advantage of MSDD for cooperative STBC using BPSK modulation over two-symbol differential detection, and

(ii) Secondly, we exploit the benefits of MSDD in the context of decision fusion in WSNs by proposing an EEDF algorithm using bandwidth efficient DAPSK modulation.

2 Energy Consumption of Cooperative MIMO using Differntial STBC

Considering a WSN of N randomly distributed nodes with node density N_D, the general communication link between the transmitter and receiver can be MIMO, Multiple-input-single-output (MISO) and Single-input-multiple-output (SIMO). The data bits are modulated into S symbols. These symbols are then mapped into a $N_T \times T$ matrix, where N_T is the number of transmitting cooperating nodes, and T is the number of channels. The number of bits per channel used is $\frac{bS}{T}$ and the transmission rate is $R = \frac{BbS}{T}$, where, B denotes the channel bandwidth and b is the number of bits used for representing a symbol. Figure 1 provides the system model considered in our work. Cooperation between N_T cooperating nodes at the transmitter end and N_R cooperating nodes at the receiving end is assumed to form a cooperative MIMO framework.

Differential STBC based on alamouti scheme[3] is used for information transmission between the cooperating nodes. The closed form BER expression for the non-coherent alamouti's scheme with BPSK modulation is given by:

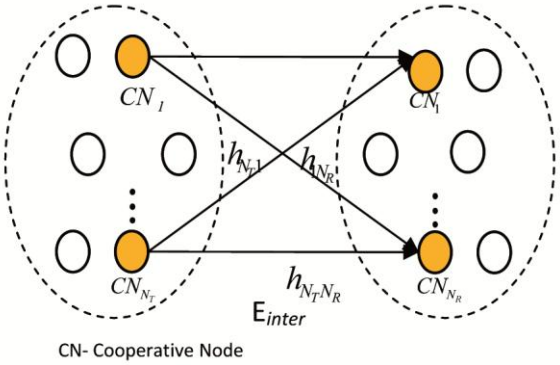

Fig. 1 — Example of geometry of WSN describing cooperative MIMO transmission using STBC.

$$P_{b\_BPSK} = \frac{1}{2}\left[1 - \sqrt{\frac{\rho}{\rho+2}} \sum_{n_R=0}^{2N_R-1} \binom{2n_R}{n_R} \left(\frac{1}{2(\rho+2)}\right)^{n_R}\right] \quad \ldots (1)$$

Where, $n_R = 0,1,\ldots N_R$, $\rho = \frac{E_{b\_STBC}^{BPSK}}{N_0}$, N_0 is the power spectral density of noise. The required $E_{b\_STBC}^{BPSK}$ for a given target BER is obtained by inverting[1]. The closed form BER expression for STBC with quadrature phase shift keying (QPSK) modulation and differential encoding and decoding is given in literature[2]. The $E_{b\_STBC}^{QPSK}$ required for a given target BER is obtained by inverting Eq. (2):

$$P_{b\_QPSK} = \frac{1}{2}\left[1 - \sqrt{\frac{\rho}{\rho+4}} \sum_{n_R=0}^{2N_R-1} \binom{2n_R}{n_R} \left(\frac{1}{\rho+4}\right)^{n_R}\right] \quad \ldots (2)$$

The total energy consumed along the signal path $E_{STBC}^{tot\_BPSK}$ is the sum of energy consumed for transmission $E_{STBC}^{t\_BPSK}$ and the energy consumed by the circuit blocks E_{STBC}^{C} is given in Eq. (3).

$$E_{STBC}^{tot\_BPSK} = E_{STBC}^{t\_BPSK} + E_{STBC}^{C} \quad \ldots (3)$$

The calculations on transmission energy are based on the link budget relationship as explained in literature[19]. Details of the transmission energy required for sending a bit for a distance d between the source and the destination for STBC using BPSK and QPSK modulation are given by Eqs (4) and (5), respectively. The circuit energy consumption is given by (6). The related circuit and system parameters used for the energy calculations are given in Table 1. The circuit parameter values are quoted from literature[12].

Table 1 — System parameters.

Symbol and value	Parameter
f_c	Carrier frequency
$G_t G_r = 5dBi$	Product of transmitter and receiver antenna gain
$P_{DAC} = 15.4mW$	Power consumption of Digital to analog converter (DAC)
$P_{ADC} = 67mW$	Power consumption of analog to digital converter (ADC)
$P_{mix} = 30.3mW$	Power consumption value of mixer
$P_{filt} = 2.5mW$	Power consumed by filters at the transmitter and receiver.
$N_f = 10dB$	Receiver noise figure
$\eta = 0.35$	Drain efficiency of RF power amplifier
$P_{syn} = 50mW$	Power consumed by frequency synthesizer
$P_{LNA} = 20mW$	Power consumption value for low-noise amplifier
$M_l = 40dB$	Link margin
λ	Wavelength
k	Path loss exponent

$$E_{STBC}^{t\_BPSK} = \frac{\zeta_h (4\pi)^2 d^k M_l N_f E_{b\_STBC}^{BPSK}}{G_t G_r \lambda^2 R} \quad \ldots (4)$$

$$E_{STBC}^{t\_QPSK} = \frac{\zeta_h (4\pi)^2 d^k M_l N_f E_{b\_STBC}^{QPSK}}{G_t G_r \lambda^2 R} \quad \ldots (5)$$

$$E_{STBC}^{C} = \frac{N_T P_{CT} + N_R P_{CR}}{R} \quad \ldots (6)$$

$$P_{CT} = P_{DAC} + P_{mix} + P_{filt} + P_{syn} \quad \ldots (7)$$

$$P_{CR} = P_{LNA} + P_{syn} + P_{mix} + P_{IFA} + P_{filt} + P_{ADC} \quad \ldots (8)$$

Similarly, the total energy consumed along the signal path using QPSK modulation $E_{STBC}^{tot\_QPSK}$ is the sum of the energy consumed for transmission $E_{STBC}^{t\_QPSK}$ given in Eq. (5) and the energy consumed by the circuit blocks E_{STBC}^{C} given in Eq. (6):

$$E_{STBC}^{tot\_QPSK} = E_{STBC}^{t\_QPSK} + E_{STBC}^{C} \quad \ldots (9)$$

3 Energy Consumption of MSDD

3.1 Energy consumption of MSDD of differential STBC

At the receiver the observation interval consists of N_w blocks. The channel during the observation interval is assumed to be constant. The approximate BER of MSDD of differential STBC with an

observation interval of three block and detecting two blocks at a time with BPSK modulation is given in Eq. (10):

$$P_{b\_MSDD\_STBC} \approx \frac{1}{2}\left[1-\mu-\frac{1}{2}\mu\left(1-\mu^2\right)\right]+\frac{1}{2}*\frac{1}{2}\left[1-\mu-\frac{1}{2}\mu\left(1-\mu^2\right)\right] \quad \ldots (10)$$

where, $\mu=\sqrt{\frac{\gamma}{\gamma+3}}$ and $\gamma=\frac{E_{b\_MSDD\_STBC}}{N_0}$. For a given target BER, $E_{b\_MSDD\_STBC}$ is obtained by inverting Eq. (10). The total energy consumed per bit under MSDD of differential STBC with BPSK modulation for three observation blocks is given in Eq. (11).

$$E_{MSDD\_STBC}^{tot}=\frac{\zeta_h(4\pi)^2 d^k M_l N_f E_{b\_MSDD\_STBC}}{G_t G_r \lambda^2 R}+\frac{N_T P_{CT}+N_R P_{CR}}{R} \quad \ldots (11)$$

3.2 MSDD-DAPSK decision fusion

The sensor nodes communicate with the fusion center over a narrowband time selective Rayleigh fading channel where the fading coefficients have an auto-correlation function $\varphi[\kappa]\cong\varepsilon\{h[n+\kappa]h^*[n]\}=J_0(2\pi f_d T_\kappa)$ where, J_0 is the zero[th] order Bessel function of the first kind and f_d is the maximum normalized Doppler frequency according to the widely used Clarke model[22]. Figure 2 refers to the reference system architecture of the proposed EEDF algorithm. To achieve bandwidth efficiency, information bits are mapped into DAPSK symbols. The DAPSK constellation involves symbols mapped onto multiple concentric rings. Figure 3 is the signal constellation diagram of 16-DAPSK. There are 2 concentric rings and each ring radius represent the 2 DASK amplitude level. There are 8 phases in each ring. If the inner ring has radius a, the outer ring has radius βa. β denotes the ring ratio of 16 DAPSK constellation.

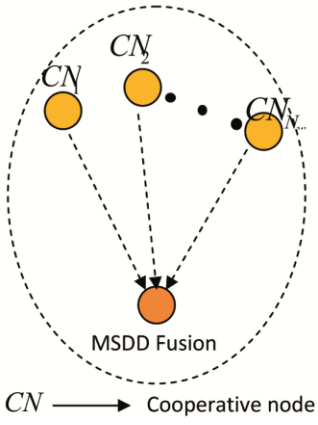

Fig. 2 — System model for MSDD decision fusion using DAPSK modulation.

The MSDD makes a decision about the i^{th} block of N_w-1 consecutively transmitted DAPSK symbols based on N_w consecutively received symbols stored in $y(i)$ given in Eq. (12).

$$y[i]=[y[i(N_w-1)],\ldots,y[(i+1)(N_w-1)]]^T \quad \ldots (12)$$

The transmitted DAPSK symbols in the i^{th} block can be expressed as in Eq. (13).

$$x[i]=[x[i(N_w-1)],\ldots,x[(i+1)(N_w-1)]]^T \quad \ldots (13)$$

Each transmitted symbol is the product of DASK symbol and DPSK symbol. The received symbol is expressed as in Eq. (14).

$$\boldsymbol{y[i]=X_d[i]h[i]+w[i]} \quad \ldots (14)$$

where, $X_d[i]=diag\{x[i]\}$, $X_d[i]=A_d[i]S_d[i]$, $A_d[i]=diag\{a[i]\}$, $S_d[i]=diag\{s[i]\}$, $a[i]$ represents the corresponding N_w consecutively transmitted constituent DASK symbols, $s[i]$ represents the corresponding N_w consecutively transmitted constituent DPSK symbols, $h[i]=[h[i(N_w-1)],\ldots,h[(i+1)(N_w-1)]]^T$ and $w[i]=[w[i(N_w-1)],\ldots,w[(i+1)(N_w-1)]]^T$ represent the fading coefficients and the Gaussian noise, respectively.

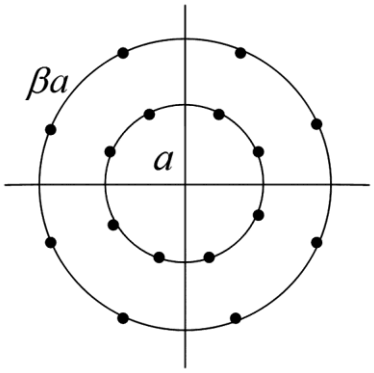

Fig. 3 — 16 DAPSK constellation.

3.3 BER analysis of MSDD-decision fusion

The probability density function (PDF) of condition on $y[i]$ can be expressed as:

$$p(y \mid X = AS) = \frac{\exp\left\{- y^H [\psi(X)]^{-1} y\right\}}{\pi^{N_W} \det[\psi(X)]} \quad \ldots (15)$$

where, $\psi(X)$ is the conditional auto correlation matrix of y.

$$\psi(X) = AS\sum_h (AS)^H + 2\sigma_N^2 I_N \quad \ldots (16)$$

where, $\sum_h$ is the auto correlation matrix of the fading process, S represents the phase matrix, A the ring-amplitude matrix, σ_N^2 is a noise variance and I_N is the $N \times N$ identical matrix. The modified maximum likelihood (ML) decision metric can be expressed as in (17). The block index i is omitted for notation simplicity.

$$\hat{x} = \underset{x \in \chi}{\arg\max} \left\{ \frac{1}{\pi^{N_W} \det[\psi(X)]} \exp\left(- y^H [\psi(X)]^{-1} y\right) \right\} \quad \ldots (17)$$

Assume that vector x is transmitted and it is decoded as vector $\hat{\boldsymbol{x}} = \hat{\boldsymbol{a}}\hat{\boldsymbol{s}}$. Based on the decision rule in Eq. (17), an error occurs if the condition given in Eq. (18) is true.

$$y^H diag\{\hat{x}\} C^{-1} diag\{\hat{x}^*\} y \le y^H diag\{x\} C^{-1} diag\{x^*\} y \quad \ldots (18)$$

where, $C \cong \varepsilon\{hh^H\} + \sigma_n{}^2 I_N$. The pair wise error probability can be derived in terms of the difference of their decoding metrics denoted by Δ. The expression (18) can be simplified as $\Delta = y^H Q y \le 0$, with $Q = diag\{\hat{x} - x\} C^{-1} diag\{\hat{x}^* - x^*\}$ Therefore, the pair wise error probability (PEP) is defined as $P(x \to \hat{x}) = P(\Delta \le 0 \mid x, \hat{x})$.

The above-mentioned probability can be computed using method depicted in literature[23]:

$$P(\Delta \le 0 \mid x, \hat{x}) \approx$$
$$-\frac{1}{q} \sum_{k=1}^{q/2} \{c\Re[\phi_\Delta(c + jc\tau_k)] + \tau_k \Im[\phi_\Delta(c + jc\tau_k)]\} \quad \ldots (19)$$

where, $\phi_\Delta(.)$ is the characteristics function of the random variable Δ and $\tau_k = \tan((2k-1)\pi/(2q))$. Also, the constant c can be set equal to one half of the smallest real parts of the poles of $\phi_\Delta(t)$ and $q = 64$ gives enough accuracy for the approximation[23]. To continue with calculating Eq. (19) the characteristics function of the random variable Δ should be determined. The characteristic function of the quadratic form $\Delta = y^H Q y$ can be expressed by Eq. (20) as given in literature[23].

$$\phi_\Delta(t) = \frac{1}{\det\{I_N + t\psi(X)Q\}} \quad \ldots (20)$$

An approximation of the bit error probability of MSDD decision fusion is obtained by evaluating Eq. (21).

$$P_{b\_MSDD}^{DAPSK} = \frac{w}{(N_w - 1)\log_2(M)} P(x \to \hat{x}) \quad \ldots (21)$$

where, w implies the hamming distance between the binary equivalent of x and $\hat{x}$ where M is the modulation order. The required $E_{b\_MSDD}^{DAPSK}$ for a target BER is obtained from Eq. (21). The total energy consumption per bit for MSDD based DAPSK can be expressed by Eq. (22).

$$E_{MSDD}^{tot\_DAPSK} = \frac{\zeta_h (4\pi)^2 d_b^k M_l N_f E_{b\_MSDD}^{DAPSK}}{G_t G_r \lambda^2 R} + \frac{N_T P_{CT} + N_R P_{CR}}{R} \quad \ldots (22)$$

3.4 Ring ratio optimization of the DAPSK constellation

The effect of the ring ratio of the DAPSK constellation on the BER has been analyzed. The value of the ring ratio that minimizes the BER evaluated using Eq. (21) is chosen as the optimum value of ring ratio denoted as β_{opt}. Figure 4 shows the impact of the ring ratio of DAPSK constellation on

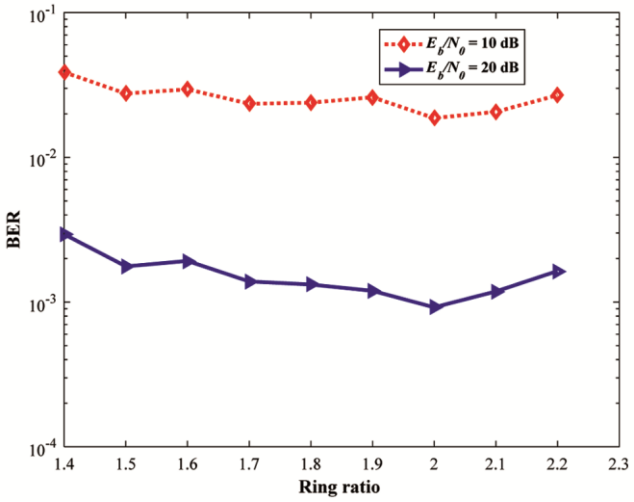

Fig. 4 — Ring ratio optimisation of DAPSK constellation.

the BER values for fixed $\frac{E_b}{N_0}$ of 10 dB and 20 dB. From the Fig. 4 it is clear that the BER is minimum at $\beta = 2$ for $\frac{E_b}{N_0}$ = 10 dB and 20 dB. Hence, β_{opt} =2 is chosen as the optimum value of ring ratio.

4 Energy Efficient Decision Fusion (EEDF) Algorithm

The pseudo code for EEDF algorithm is presented below. The algorithm aims at minimizing the total energy consumption per bit by optimally choosing the ring ratio of the DAPSK constellation and also by processing multiple symbols at a time. In step 1, the parameters required for the calculation of the total energy consumption such as, N_T, ζ_h, d, M_l, G_t, N_R, P_{CT}, N_f, G_r, λ^2, R, P_{CR} is initialized. In step 2, the optimal ring ratio of the DAPSK constellation that minimizes the BER is found. The relation between the required $\frac{E_b}{N_0}$ for a target BER is obtained in step 3. The total energy consumed per bit at various transmission distances for a target BER is found in step 4.

5 Simulation Results

Figure 5 depicts the BER values for different $\frac{E_b}{N_0}$ for $N_T = 2$ and N_R cooperative node at the receiver using BPSK modulation. From Fig. 5 show increasing the number of cooperative nodes at the receiver from 1 to 2 providing a gain of 7 dB in $\frac{E_b}{N_0}$ for a BER of 10^{-3}. Furthermore, compared to the coherent case the differential method suffers a loss of 3 dB in $\frac{E_b}{N_0}$. Figure 6 represents the BER values for different values of $\frac{E_b}{N_0}$ for $N_T = 2$, and N_R cooperative node at the receiver using QPSK modulation. Figure 6 shows that for a BER of 10^{-3}, the differential STBC with two transmitter nodes and one receiver node requires $\frac{E_b}{N_0}$

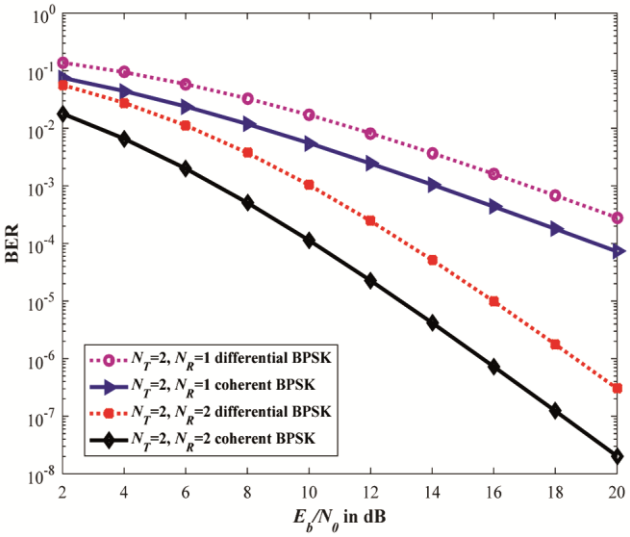

Fig. 5 — BER versus $\frac{E_b}{N_0}$ for STBC using BPSK modulation.

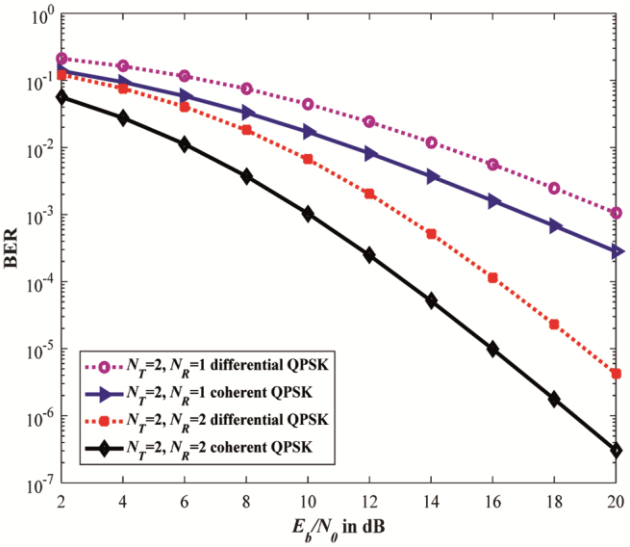

Fig. 6 — BER versus $\frac{E_b}{N_0}$ for STBC using QBPSK modulation.

Algorithm: Energy Efficient Decision Fusion (EEDF) algorithm

1 Initialize: The parameters required for energy consumption such as N_w, M, f_D and the system parameters given in Table I

2 Find the optimum ring ratio that minimizes the BER using Eq. (21)

3 Evaluate $P_{b\_MSDD}^{DAPSK}$ based on Eq. (21) for β_{opt} and then invert $P_{b\_MSDD}^{DAPSK}$ to get the required value of $E_{b\_MSDD}^{DAPSK}$

4 Calculate the total energy consumption per bit using Eq. (22), for various transmission distances.

of 20 dB. Increase in the number of receiver node to two requires $\frac{E_b}{N_0}$ of 13 dB. The differential transmission requires an extra 3 db $\frac{E_b}{N_0}$ for achieving the same BER compared to coherent transmission. Table 2 summarizes the simulation results of the required $\frac{E_b}{N_0}$ for coherent and differential STBC using BPSK and QPSK modulation.

The variations in energy consumption for differential STBC using BPSK modulation for cooperative MIMO configuration and cooperative MISO configuration are shown in Fig. 7. The energy saving from the proposed method is calculated using the formula $\frac{E_{exsisting}-E_{proposed}}{E_{exsisting}}$. Figure 7 shows that at transmission distance of 100 m between the transmitting and receiving cooperative nodes, the energy saving obtained by cooperative MIMO configuration by applying differential STBC is 80 % compared to differential STBC cooperative MISO configuration. The coherent cooperative MIMO configuration achieves an energy saving of 33.33 % compared to differential cooperative MIMO configuration.

The variations in energy consumption of differential STBC using QPSK modulation for cooperative MIMO configuration and cooperative MISO configuration are shown in Fig. 8. Figure 8 shows that, at a transmission distance of 100 m between transmitting and receiving cooperative nodes, the energy saving obtained by cooperative MIMO configuration is 79.31 % compared to differential STBC cooperative MISO configuration. The coherent cooperative MIMO configurations achieve a total energy saving of 50 % compared to differential cooperative MIMO configuration. Table 3 compares the total energy consumption per bit of coherent and differential STBC for varying N_R using BPSK and QPSK modulation.

Table 2 — Comparison of the required $\frac{E_b}{N_0}$ between coherent and differential stbc using bpsk and qpsk modulation.

Modulation	Required $\frac{E_b}{N_0}$ in dB for BER of 10^{-3}			
	Coherent		Differential	
	N_T=2 & N_R =1	N_T =2 & N_R =2	N_T =2 & N_R =1	N_T =2 & N_R =2
BPSK	14	7	17	10
QPSK	17	10	20	13

Table 3 — Energy consumption per bit comparison between coherent and differential stbc for varying N_R using bpsk and qpsk modulation.

Modulation	Energy consumed per bit at 100 m distance			
	Coherent		Differential	
	N_T =2 & N_R =1	N_T =2 & N_R =2	N_T =2 & N_R =1	N_T =2 & N_R =2
BPSK	0.0008	0.0002	0.0015	0.0003
QPSK	0.0015	0.0003	0.0029	0.0006

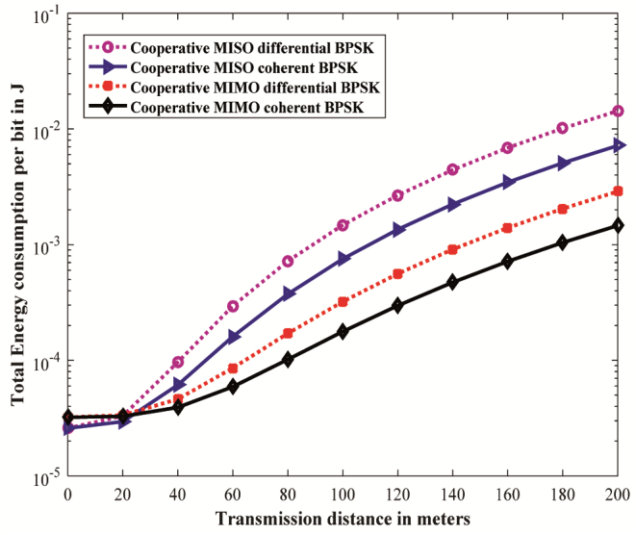

Fig. 7 — Total energy consumption per bit of differential STBC using BPSK modulation versus distance for cooperative MISO and cooperative MIMO configuration.

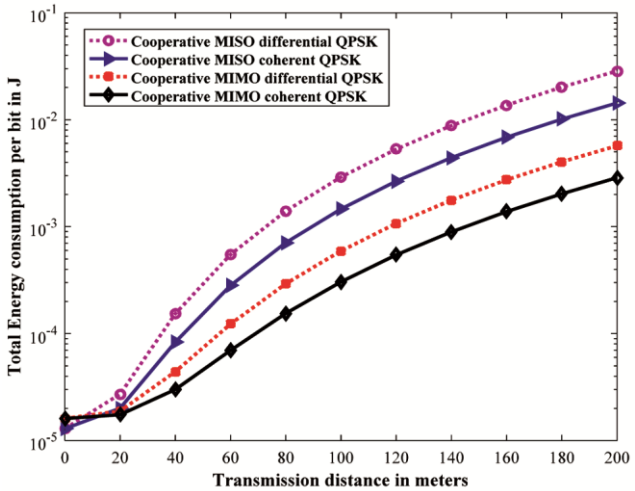

Fig. 8 — Total energy consumption per bit of differential STBC using QPSK modulation versus distance for cooperative MISO and cooperative MIMO configuration.

Figure 9 depicts the BER versus the $\frac{E_b}{N_0}$ plot for differential STBC with MSDD using BPSK modulation.

From the Fig. 9, it is observed that 17.1 dB of $\frac{E_b}{N_0}$ is required for differential STBC with 2 block whereas, only 16.8 dB of $\frac{E_b}{N_0}$ is required when the block size is increased to three.

Thus, a gain of about 0.3 dB $\frac{E_b}{N_0}$ is achieved by increasing block size to three. Figure 10 presents the energy consumption per bit comparison between MSDD differential STBC for the various blocks.

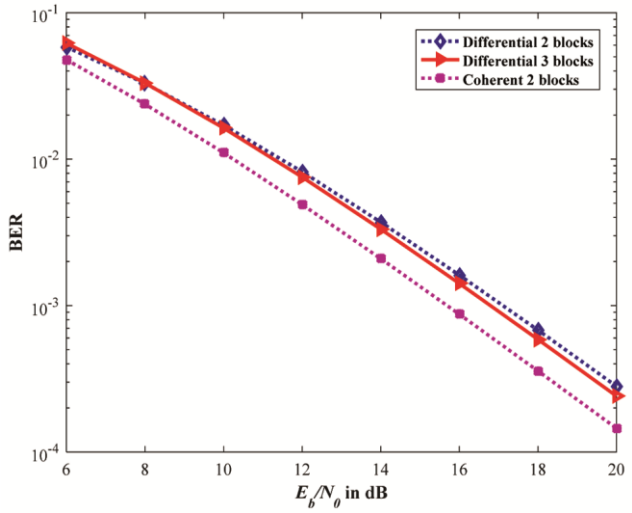

Fig. 9 — BER versus for MSDD of STBC.

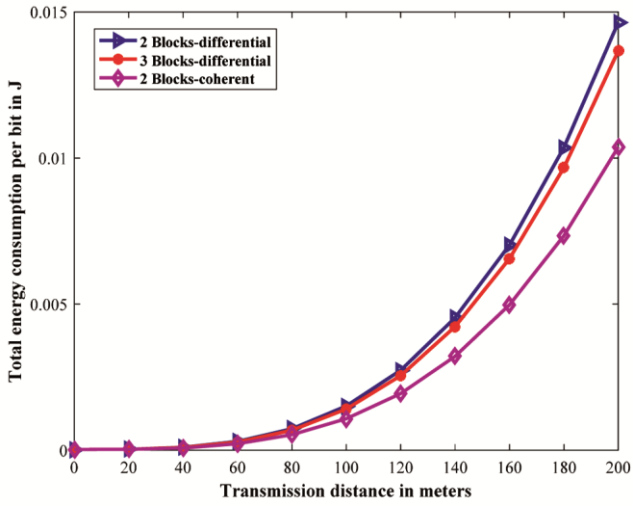

Fig. 10 — Total energy consumption per bit of MSDD differential STBC using BPSK modulation versus distance for cooperative MISO configuration.

From Fig. 10 it is noted that, at a difference of 120 m between transmitting and receiving nodes the MSDD with three blocks provides significant energy saving of about 6.61 % compared to two block MSDD for STBC. Table 4 shows the comparison of the total energy consumption per bit for differential STBC MSDD with block size two and block size three. A reduced-complexity design for the soft-decision MSDSD was proposed by Chao Xu *et al.*[24]. The design demonstrated the outperformance of the MSDSD aided Differential Quadrature Amplitude Modulation (DQAM) over its DPSK counterpart. The disadvantage is that the detection complexity of DQAM relying on Multiple Amplitude (MA)-ring Star Quadrature Amplitude Modulation (QAM) constellation is at least about MA times higher than that of its DPSK counterpart. They showed that MSDSD aided DPSK is an eminently suitable candidate for turbo detection assisted coded systems operating at high Doppler frequencies.

The BER for different values of $\frac{E_b}{N_0}$ for the proposed EEDF algorithm are illustrated in Fig. 11.

Table 4 — Comparison of total energy consumption per bit for differential stbc msdd with block size two and block size three.

Distance in meters	Total energy consumed per bit in Joules for a BER of 10^{-3}		
	Differential STBC 2 Blocks	Differential STBC 3 Blocks	Energy saving
120	0.002735	0.002554	6.61
140	0.004532	0.004231	6.64
160	0.007027	0.00656	6.64

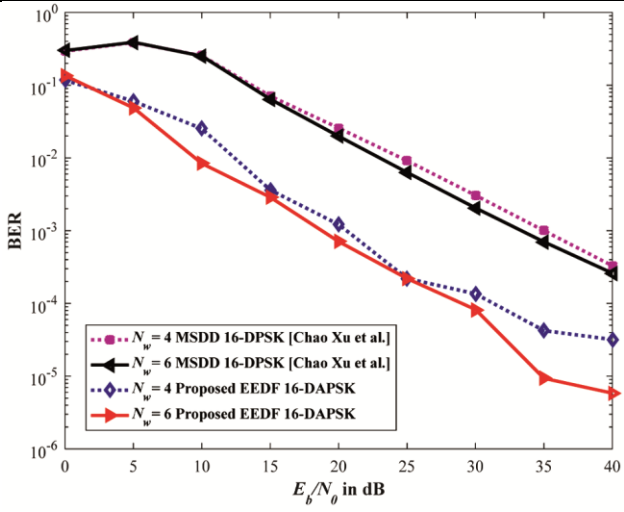

Fig. 11 — BER performance of the proposed EEDF algorithm based on 16 DAPSK and MSDD aided 16 DPSK for different window size N_W and normalized Doppler frequency f_d =0.03.

The proposed EEDF algorithm is compared with 16 DPSK method[24]. Optimized ring ratio β_{opt}=2 that minimizes the probability of error for DAPSK constellation is used in the proposed algorithm. Figure 11, shows the performance of the MSDD based 16 DAPSK fusion as better than MSDD 16 DPSK for window size N_W=2 and N_W=4. For a BER of 10^{-3} there is a gain of approximately 10 dB for the proposed method compared to 16 DPSK decision fusion. Moreover, the BER decreases with increase in window size N_W. From the figure it is clear that for a BER of 10^{-3}, increasing N_W in the proposed method from 4 to 6 results in approximately 5 dB gain in $\frac{E_b}{N_0}$.

Table 5 shows the comparison of the BER values of the proposed EEDF algorithm based on 16 DAPSK and MSDD aided 16 DPSK for different window size N_W and normalized Doppler frequency f_d =0.03.

The variations in total energy consumption with the transmission distance for the proposed EEDF algorithm are depicted in Fig. 12. Figure 12 shows that, at a distance of 100 m between transmitting and receiving nodes invoking the EEDF algorithm provides significant energy saving of about 89 % compared to decision fusion based on 16 DPSK for N_W = 6.

6 Network Lifetime Analysis

Network lifetime is the duration for which the network is fully operative. The network lifetime is determined in terms of number of rounds the information is transmitted until the first node runs out of energy. At the beginning of simulation, each node is equipped with energy of 10 joule. The lifetime of the network for both the DPSK MSDD decision fusion and EEDF algorithm are computed for N_W = 4 and N_W = 6 for different distance between transmitting and fusion center and is shown in Fig. 13. The maximum distance for our simulation is 200 m. The Fig. 13 shows, the lifetime of the proposed EEDF algorithm as higher than DPSK MSDD scheme for all the distances. As the transmission distance increases, the lifetime of network decreases. The most important parameters that measure the performance of fast fading channel are the Level crossing rate (LCR),

Table 5 — BER vales of the proposed EEDF algorithm based on 16 DAPSK and MSDD aided 16 DPSK for different window size N_W and normalized doppler frequency f_d =0.03.

$\frac{E_b}{N_0}$ in dB	BER			
	$N_W = 4$		$N_W = 6$	
	16 DPSK	Proposed EEDF 16 DAPSK	16 DPSK	Proposed EEDF 16 DAPSK
0	0.29238	0.11724	0.29868	0.135101
5	0.38626	0.060186	0.38945	0.048717
10	0.25421	0.025251	0.25156	0.008404
15	0.07086	0.003629	0.06429	0.002881
20	0.02574	0.001216	0.01985	0.000708
25	0.00915	0.00022	0.00632	0.00022

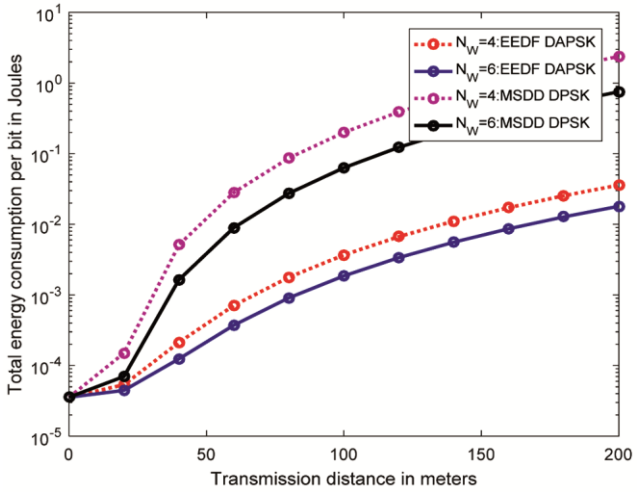

Fig. 12 — Energy consumption per bit comparison between proposed EEDF algorithm based on 16 DAPSK and MSDD 16 DPSK technique for N_W = 4 and N_W = 6 for different distance between transmitting and fusion center.

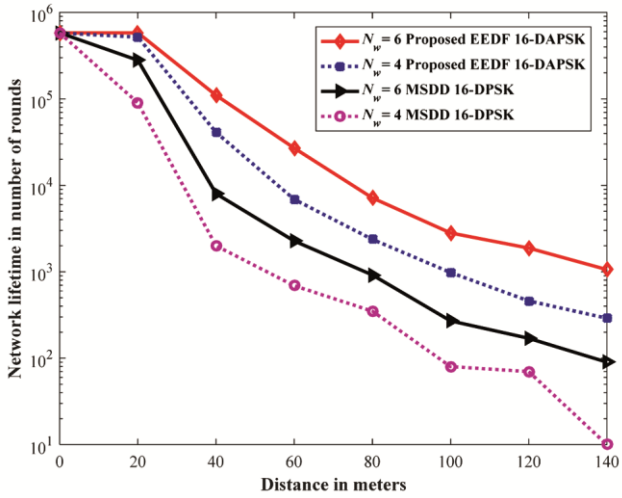

Fig. 13 — Network lifetime comparison between proposed EEDF algorithm based on 16 DAPSK and MSDD 16 DPSK technique for N_W = 4 and N_W = 6 for different distance between transmitting and fusion center.

Average fade duration (AFD) and BER. The LCR is defined as the rate at which the signal envelope crosses a specified level in the positive slope. AFD is the time duration that the fading envelope remains below a specified level. The typical values of LCR and AFD for fast fading channel assuming a speed of 100 Kmph is 225.6 and 7.0264×10^{-5}, respectively.

7 Conclusions

A comprehensive analytical model has been developed for demonstrating the benefits of MSDD for differential STBC in WSN's. An EEDF algorithm has been proposed for WSN's. The algorithm exploits the benefits of spectrally efficient DAPSK modulation and multiple symbol differential detection. The key idea behind the algorithm is the ring ratio optimization of the DAPSK constellation that reduces the probability of error. Extensive simulations show the benefits of increasing the differential detection window size, which is particularly useful in fast fading channel conditions when achievement of channel estimation is a difficult proposition.

References

1 Akyildiz I F, Su W, Sankarasubramaniam Y & Cayirci E, *Comput Netw*, 38 (2002) 393.

2 Paul H & Dominic F, *Error Performance of Multiple symbol Differential Detection of PSK Signal Transmitted over Correlated Rayleigh Fading Channels*, (1991) 568.

3 Alamouti S, *IEEE J Select Areas Commun*, 16 (1998) 1451.

4 Gao C & Haimovich A M, *IEEE Commun Lett*, 7 (2003) 314.

5 Weifeng S & Xiang G X, *IEEE Trans IT*, 50 (2004) 2331.

6 Hongbin L & Tao L, *Digital Signal Process*, (2006) 261.

7 Chunjun G & Alexander M, *IEEE Trans Commun*, 54 (2006) 1502.

8 Hwang C S, Nam J C & Tarokh V, *IEEE Trans Signal Process*, 51 (2003) 2955.

9 Chow Y C, Nix A R & McGeehan J P, *Analysis of 16-APSK Modulation in AWGN and Rayleigh Fading Channel*, 28 (1992) 1606.

10 Wang L & Hanzo L, *IEEE Trans Vehicul Technol*, 61 (2012) 894.

11 Shinya S, Chao X, Soon Xin N & Lajos H, *IEEE Trans Commun*, 59 (2011) 3426.

12 Shuguang C, Goldsmith A J & Ahmad B, 22 (2004) 1089.

13 Yong Y, Zhihai H & Min C, *IEEE Trans Vehicul Technol*, 50 (2006) 856.

14 Faouk F, Rizki R & Fayez W, *IET Wireless Sens Syst*, 4 (2014) 159.

15 Zhang J, Fei L, Gao Q & Peng X H, *IEEE Trans Wireless Commun*, 10 (2011) 3090.

16 Chung J M, Hyung K J & Han D, *IEEE Trans Vehicul Technol*, 61 (2012) 4069.

17 Nguyen D N & Krunz M A, *ACM Trans Sens Net*, 10 (2014) 1.

18 Lei A & Schober R, *IEEE Trans Wireless Commun*, 9 (2004) 778.

19 Proakis J G, Digital Communications, 4th Edn New York, McGraw-Hill, (2000).

20 Kumar S & Amutha R, *KSII Trans Internet Inform Syst*, 10 (2016) 3080.

21 Kanthimathi M, Amutha R & Kumar S, *Clust Comput*, https://doi.org/10.1007/s10586-017-1688-4-y(2017).

22 Hanzo L, Akhtman Y, Wang L & Jiang M, MIMO-OFDM for LTE, WIFI and WIMAX: Coherent versus Non-Coherent and Cooperative Turbo-Transceivers, John Wiley and IEEE Press, 2010.

23 Biglieri E, Caire G, Taricco G & Ventura-Traveset J, *Electron Lett*, 32 (1996) 191.

24 Xu C, Liang D, Ng S X & Hanzo L, *IEEE Trans Vehicul Technol*, 62 (2013) 2633.